Environmental Science & Technology

Article

pubs.acs.org/est

Uptake, Translocation, and Transformation of Quantum Dots with Cationic versus Anionic Coatings by *Populus deltoides* × *nigra* Cuttings

Jing Wang,[†] Yu Yang,[†] Huiguang Zhu,[‡] Janet Braam,[§] Jerald L. Schnoor,[∥] and Pedro J. J. Alvarez*[,†]

[†]Department of Civil & Environmental Engineering, [‡]Department of Chemistry, and [§]Department of Biochemistry & Cell Biology, Rice University, Houston, Texas 77005, United States

[∥]Department of Civil & Environmental Engineering, University of Iowa, Iowa City, Iowa 52242, United States

Supporting Information

ABSTRACT: Manipulation of the organic coatings of nanoparticles such as quantum dots (QDs) to enhance specific applications may also affect their interaction and uptake by different organisms. In this study, poplar trees (*Populus deltoides* × *nigra*) were exposed hydroponically to 50-nM CdSe/CdZnS QDs coated with cationic polyethylenimine (PEI) (35.3 ± 6.6 nm) or poly(ethylene glycol) of anionic poly(acrylic acid) (PAA-EG) (19.5 ± 7.2 nm) to discern how coating charge affects nanoparticle uptake, translocation, and transformation within woody plants. Uptake of cationic PEI-QDs was 10 times faster despite their larger hydrodynamic size and higher extent of aggregation (17 times larger than PAA-EG-QDs after 11-day incubation in the hydroponic medium), possibly due to electrostatic attraction to the negatively charged root cell wall. QDs cores aggregated upon root uptake, and their translocation to poplar shoots (negligible for PAA-EG-QDs and 0.7 ng Cd/mg stem for PEI-QDs) was likely limited by the endodermis. After 2-day exposure, PEI and PAA-EG coatings were likely degraded from the internalized QDs inside the plant, leading to the aggregation of the metallic cores and a "red-shift" of fluorescence. The fluorescence of PEI-QD aggregates was stable inside the roots through the 11-day exposure period. In contrast, the PAA-EG-QD aggregates lost fluorescence inside the plant after 11 days probably due to destabilization of the coating, even though these QDs were stable in the hydroponic solution. Overall, these results highlight the importance of coating properties in the rate and extent to which nanoparticles are assimilated by plants and potentially introduced into food webs.

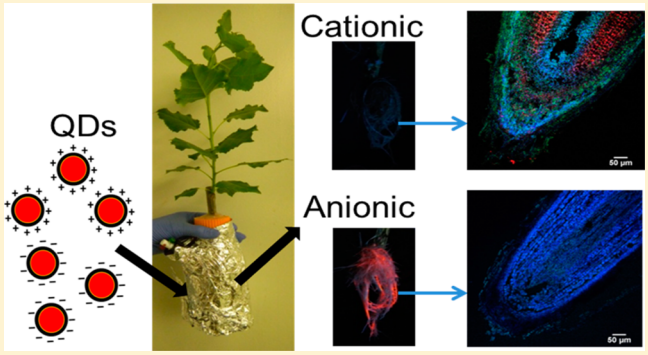

INTRODUCTION

Quantum dots (QDs) are semiconductor nanoparticles (NPs) that offer valuable functionality for cellular labeling, drug delivery, solar cells, and quantum computation.[1−3] Their fluorescent properties are particularly useful for bioimaging,[4] making them convenient models to visualize NP uptake by a wide variety of organisms.[1,5−8] QDs typically consist of a metallic core (typically CdSe, CdTe, ZnSe, or PbSe) surrounded by a zinc or cadmium sulfide shell that is coated by a polymer that mitigates aggregation and stabilizes the core.[4,9] Manipulation of this organic coating (e.g., by modulating charge or hydrophobicity, or by including recognition agents such as antibodies) can influence their physicochemical properties and enable more targeted delivery for biomedical imaging and photothermal therapy.[4,10,11] When QDs or other NPs are incidentally or accidentally released to ecosystems, their surface coatings could also modulate their mobility and uptake by different organisms, such as plants.

Discerning how NP coatings affect their accumulation and fate in plants is critical for understanding uptake and translocation processes as well as mitigating NP bioaccumulation and introduction into food webs. Some studies have investigated the vegetative uptake and translocation of various NPs (e.g., Au,[12−14] Al,[15] CeO_2,[16,17] and TiO_2[18,19]) and NP translocation to reproductive organs has also been reported.[20,21] However, very few studies have considered the effect of coatings on this process.[12,22] Zhu et al. exposed four different herbaceous plants to Au NPs coated by polymers with the same inside functional groups (alkanethiol and ethylene groups) but different terminal functional groups (i.e., amino, hydroxyl or carboxyl groups).[12] They found that positively charged NPs were most efficiently taken up by roots, while negatively charged NPs showed the highest translocation potential even though they had the lowest tendency to accumulate in roots. Easier translocation of anionic than

Received: March 24, 2014
Revised: May 19, 2014
Accepted: May 28, 2014
Published: May 28, 2014

   dx.doi.org/10.1021/es501425r | Environ. Sci. Technol. 2014, 48, 6754−6762

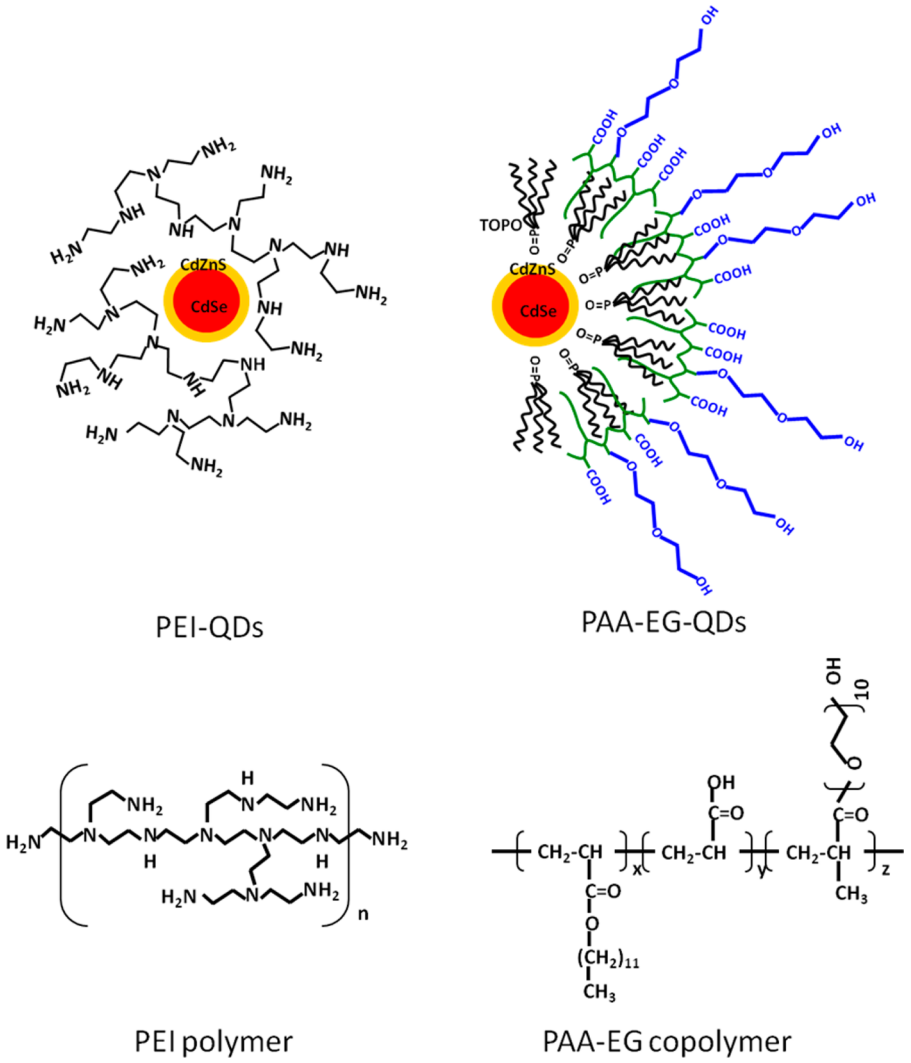

Figure 1. Structure of QDs and the coating polymers. QDs contain a CdSe core and a CdZnS shell, which are coated with cationic polyethylenimine (PEI) or poly(ethylene glycol) of anionic poly(acrylic acid) (PAA-EG).

cationic Au NPs was also observed for rice after 5-day or 3-month hydroponic exposure.[22] Nevertheless, the mechanisms by which different coating properties affect NP plant uptake through roots and subsequent translocation remain poorly understood. Moreover, it is unknown whether the uptake and translocation of NPs by woody trees, which have woody roots and stems and well-defined vascular system, follow the same trends as for herbaceous plants. This is a critical knowledge gap, because woody plants are the primary producers in most terrestrial ecosystems.

When plants take up xenobiotic compounds, they can detoxify or compartmentalize the contaminants through various biochemical processes.[23,24] Plant response can often be correlated to the physicochemical properties of the foreign substances, such as hydrophilicity.[25,26] Biotransformation of various NPs within plants, including CuO,[27,28] TiO_2,[18] ZnO,[27,29] $Ni(OH)_2$,[30] La_2O_3,[31] Yb_2O_3[32] and CeO_2[20,33] has been reported. Whereas these studies confirmed NP transformations using advanced spectroscopic methods such as X-ray scanning transmission microscopy (STXM) and X-ray absorption near edge structure (XANES) analysis, it is unclear how the mechanisms, rate, and extent of phytotransformation were influenced by NP coating properties.

In this study, we characterized the uptake and translocation of CdSe/CdZnS QDs by woody poplar trees and compared the effects of cationic versus anionic organic coatings on these processes, using confocal microscopy. This technique has been widely used to visualize the uptake of QDs by different organisms.[1,6,34,35] Spectral imaging, which has been proven effective for separating the QDs fluorescence signal from tissue autofluorescence,[1] was also used to investigate QD distribution inside the plant. We also investigated how the charge of the QD coating affects uptake and translocation dynamics by quantifying the internalized Cd and Se concentrations at different time points. Transformation of QDs was explored by analyzing the QD spectral profiles.

MATERIALS AND METHODS

QDs Characterization and Stability Test. CdSe/CdZnS QDs coated with cationic (ζ = 25.7 ± 3.9 mV) polyethylenimine (PEI) or poly(ethylene glycol) of anionic (ζ = −21.3 ± 1.2 mV) poly(acrylic acid) (PAA-EG) (Figure 1) were synthesized as described before.[5,6,36,37] Both QDs have similar uniform core size (4 nm), shape, and stability in distilled water as shown by TEM image (Figure S1). Their metal contents were also comparable as determined by ICP-MS after

dx.doi.org/10.1021/es501425r | Environ. Sci. Technol. 2014, 48, 6754−6762

70% HNO_3 (trace metal grade) digestion at 90 °C for 2 h. One nanomole of PEI-QDs contains 70.5 ± 0.6 μg Cd, 45.0 ± 0.9 μg Zn, and 17.8 ± 0.4 μg Se, while that for PAA-EG-QDs was 78.1 ± 0.8 μg Cd, 41.4 ± 0.1 μg Zn, and 27.4 ± 2.0 μg Se, respectively.

Stability of the QDs in plant growth medium (1/4-strength Hoagland solution) was monitored for 11 days. Zeta-potential and hydrodynamic size of QDs were measured by a Zen 3600 Zetasizer Nano (Malvern Instruments, UK) (Table 1). To monitor the dissolution of Cd and Se from QDs in 1/4-strength Hoagland solution, samples were taken at several time points (day 0, 1, 2, 5, and 11), and released Cd/Se ions were separated using Amicon ultra centrifugal filters (molecular weight cutoff 10,000, Millipore, MA, USA). Cd and Se ion concentrations in the filtrate were analyzed by an Elan 9000 ICP-MS (PerkinElmer, Waltham, MA, USA). Details on ICP-MS analysis are provided in the Supporting Information. Fluorescence spectra of QDs were obtained on an Infinite M1000 microplate reader (Tecan, Switzerland). All the stability tests were prepared in triplicate.

Table 1. Zeta Potential and Hydrodynamic Size of PEI-QDs and PAA-EG-QDs before and after 11-day Incubation in 1/4-Strength Hoagland Solution[a]

	PEI-QDs	PAA-EG-QDs
ζ-potential day 0	25.7 ± 3.9 mV	−21.3 ± 1.2 mV
ζ-potential day 11	23.3 ± 1.7 mV	−18.8 ± 1.6 mV
hydrodynamic size day 0	35.3 ± 6.6 nm	19.5 ± 7.2 nm
hydrodynamic size day 11	683.8 ± 89.1 nm*	40.9 ± 22.0 nm

[a]Asterisks (*) denote the statistically significant ($p < 0.05$) changes of ζ-potential or hydrodynamic size on day 11 compared to day 0. For all the tests, $n = 3$ and values are averages ±1 standard deviation.

Poplar Growth and Exposure Method. Eight-inch poplar cuttings from male clones of the adult hybrid poplar trees (*Populus deltoides* × *nigra*, DN-34, Segal Ranch, WA, USA) were grown in 1/4-strength Hoagland solution (pH 6.8)[38] for one month. Healthy samples with similar lengths of shoots and roots were selected to conduct the exposure experiment as described before.[39] Briefly, poplar cuttings were placed in a 500 mL glass exposure reactor filled with 1/4-strength Hoagland solution (pH 6.8, 400 mL) containing 50 nM PEI-QDs or PAA-EG-QDs. Controls were prepared identically without QDs. Evapotranspiration from each tree, which is a major driver

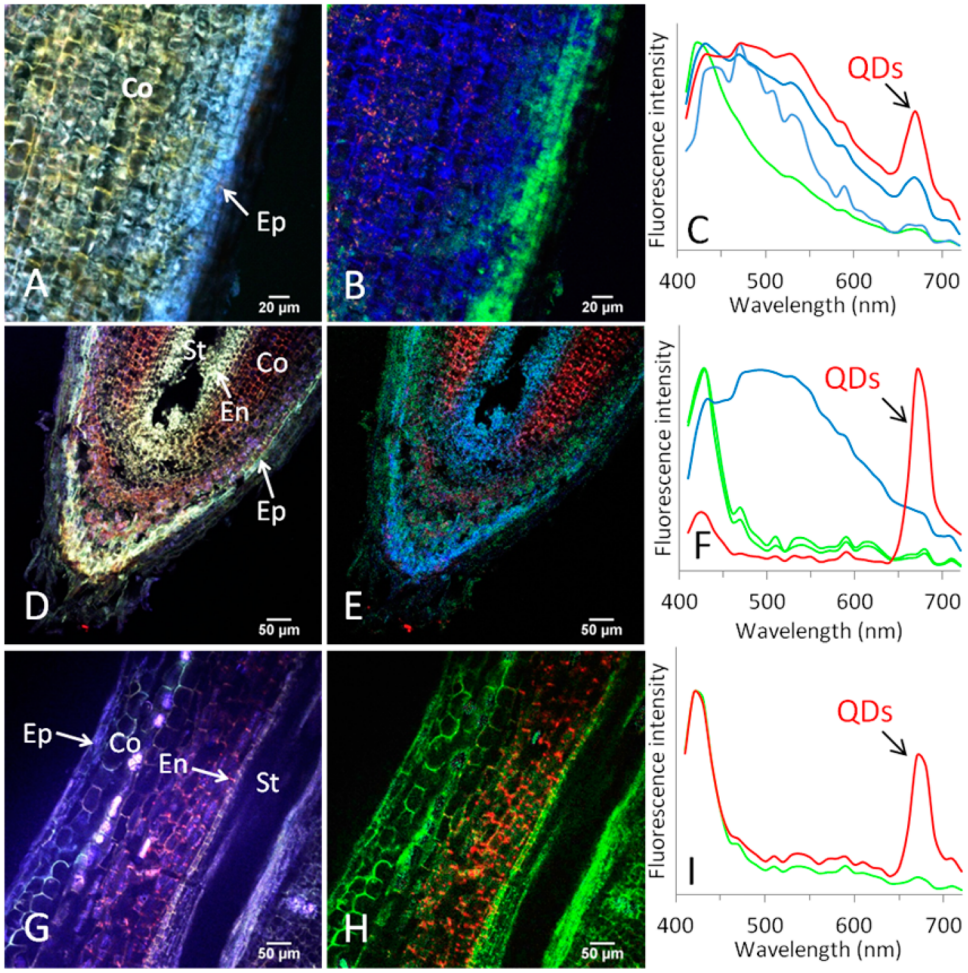

Figure 2. Distribution of PEI-QDs in longitudinal sections of poplar root after 2-day exposure (A) as well as in root tip (D) and root (G) after 11-day exposure. The spectral unmixed images (B, E, H) of these three original fluorescence images (A, D, G) were obtained based on the blind spectral unmixed analysis (C, F, I). In the spectral unmixed images (B, E, H), PEI-QDs fluorescence is shown in red and plant autofluorescence in green and blue. In blind spectral unmixed analysis results (C, F, I), PEI-QDs fluorescence spectrum is shown in red and plant autofluorescence spectra in green and blue. Due to aggregation of the QDs cores, the unmixed QDs emission peak red-shifted to 670 nm, which is probably the highest emission wavelength for CdSe type of QDs. Tissues: epidermis (Ep), cortex (Co), endodermis (En), stele (St). Bars: 20 μm (A, B), 50 μm (D, E, G, H).

dx.doi.org/10.1021/es501425r | Environ. Sci. Technol. 2014, 48, 6754−6762

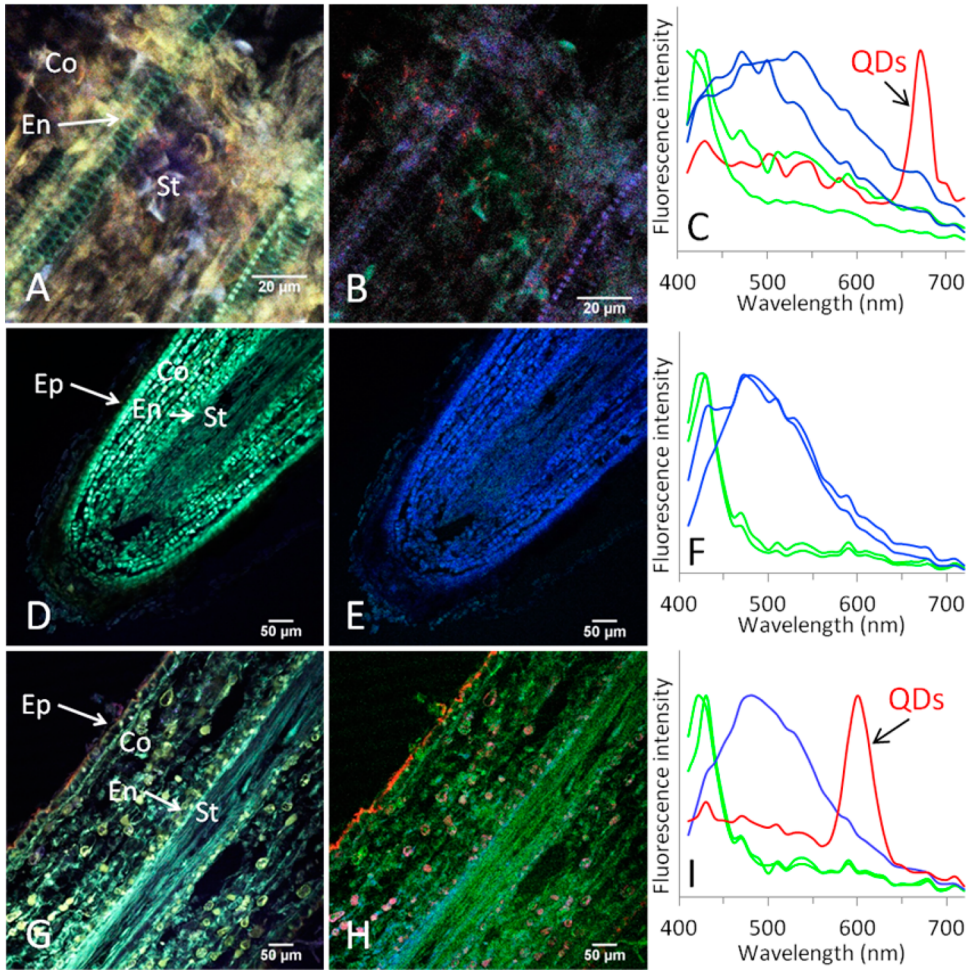

Figure 3. Distribution of PAA-EG-QDs in longitudinal sections of poplar root after 2-day exposure (A) as well as in root tip (D) and root (G) after 11-day exposure. The spectral unmixed images (B, E, H) of these three original fluorescence images (A, D, G) were obtained based on the blind spectral unmixed analysis (C, F, I). In the spectral unmixed images (B, E, H), PAA-EG-QDs fluorescence is shown in red and plant autofluorescence in green and blue. In blind spectral unmixed analysis results (C, F, I), PAA-EG QDs fluorescence spectrum is shown in red and plant autofluorescence spectra in green and blue. Due to aggregation of the QDs cores after 2 day exposure, the unmixed QDs emission peak red-shifted to 670 nm (C), which is probably the highest emission wavelength for CdSe type of QDs. Tissues: epidermis (Ep), cortex (Co), endodermis (En), stele (St). Bars: 20 μm (A, B), 50 μm (D, E, G, H).

for uptake, was monitored daily by weighing the whole reactor, and DI water was added to replace the solution loss except the fifth day. On the fifth day, 1/4-strength Hoagland solution instead of DI water was used to compensate for the nutrient loss. Fluorescence images of roots were taken for each treatment at various time points (4 h, 2 day, and 11 day) under a UV lamp (Figure S2). Plants were harvested after either 2- or 11-day exposure, and different plant tissues (root, stem, and leaf) were separated and weighed at harvest. Roots were washed with 100 mL DI water to remove the QDs loosely attached on root surface, and the rinse solution was collected for ICP-MS analysis. Then, plant tissues were dried at 90 °C for at least 2 days to reach constant weight.

Confocal Microscopy. To investigate the uptake of QDs by poplar roots, longitudinal sections of QDs exposed roots were prepared and analyzed with confocal microscopy. Two samples from two poplar trees were prepared for each treatment. Main root tip samples (around 1 cm long) were taken after 2- and 11-day hydroponic exposure to QDs. Fresh samples were fixed immediately in fixative (4% paraformaldehyde solution) and kept under vacuum for 15 min, following by 2-h fixation at 4 °C. After two washes with phosphate buffered saline (PBS), samples were moved into fresh fixative and left overnight at 4 °C. On the second day, samples were infiltrated in 10% and 20% sucrose solution, following by embedding in optimum cutting temperature (O.C.T.) compounds. Longitudinal sections (20 μm) were cut with a cryostat (Leica CM 1850 UV, Germany) and collected on Superfrost Plus glass slides covered with cover glasses. The mounting medium was Prolong Gold antifade reagents (Life Technologies Corporation, CA, USA). All other chemicals were bought from Electron Microscopy Sciences (PA, USA). Imaging was performed on a Nikon A1-Rsi confocal system (Japan) using spectral detector (SD), as detailed in the Supporting Information.

Statistical Analysis. Whether the accumulation of Cd and Se in QDs exposed poplar tissues was significant compared to that in controls was determined by Student's *t*-test at the 95% confidence level.

RESULTS AND DISCUSSION

Most manufactured nanoparticles (NPs) are synthesized with surface coatings that enhance their biocompatibility, stability,

dx.doi.org/10.1021/es501425r | *Environ. Sci. Technol.* 2014, 48, 6754−6762

and usefulness. Such coatings reduce NP aggregation and precipitation, mitigate the release of potentially toxic constituents, and modulate NP mobility when released into biological or environmental systems.[40−46] Yet, the influence of coatings (and their associated surface charge) on NP uptake, biotransformation, and bioaccumulation by terrestrial organisms has received limited attention in the literature, which motivated this study.

Cationic PEI-QDs Were Taken up Faster than Anionic PAA-EG-QDs by Poplar Roots. QD fluorescent signals were detected after 2 days in the longitudinal sections of poplar roots exposed to PEI-QDs or PAA-EG-QDs (Figure 2A-B and 3A-B), but not in untreated controls (Figure S3), demonstrating plant uptake of QDs. Some PAA-EG-QDs reached the stele possibly through the endodermis (Figure 3A-B). It is unlikely that these QDs entered at the root tip, where the casparian strip is not formed,[47] since the PAA-EG-QDs fluorescence signal was not detected in the root tip after 2-day exposure (Figure S4).

Positively charged PEI-QDs were adsorbed and/or assimilated by the roots faster than negatively charged PAA-EG-QDs, resulting in faster removal from the hydroponic medium (Figure 4A and Table 2) even though PEI-QDs had a larger hydrodynamic size and aggregated to a higher extent in the exposure medium (Table 1). Differences in evapotranspiration cannot explain the faster uptake of PEI-QDs since the 11-day cumulative evapotranspiration of poplars exposed to these QDs was slightly lower than for poplars exposed to PAA-EG-QDs and significantly lower ($p < 0.05$) than for untreated controls (Figure S5), suggesting these poplars were under stress. However, the fresh biomass and dry biomass of different poplar tissues were not affected by QDs exposure (data not shown). Apparently, the difference in uptake rates of the two types of QDs was influenced mainly by differences in their surface charge. The plant cell wall is negatively charged because it contains high concentrations of uronic acids.[48,49] Electrostatic attraction between the root cell wall and the cationic PEI-QDs may facilitate adsorption on the root epidermis and subsequent uptake. In contrast, electrostatic repulsion between root surface and anionic PAA-EG-QDs may slow down the uptake process. This is consistent with Au NP uptake studies by different herbaceous plants,[12,22] which found that cationic Au NPs were most readily taken up than neutral or anionic Au NPs. Thus, electrical potential is an important uptake driving force for NPs with ionized coatings interacting with both woody and herbaceous plants in hydroponic systems.

Consistent with faster uptake of cationic QDs, poplar roots accumulated Cd and Se at significantly higher concentrations following 2-day exposure to larger PEI-QDs (2286 ± 174 ng Cd/mg root, 902 ± 100 ng Se/mg root) than to PAA-EG-QDs (157 ± 55 ng Cd/mg root, 62 ± 15 ng Se/mg root) (Figure 4A, $p < 0.05$). Accordingly, only 37 ± 17% of the total added Cd remained in the hydroponic solution after 2-day exposure to PEI-QDs, compared to 91 ± 2% for PAA-EG-QDs (Table 2). For both QD treatments, the amount of Cd released as ions in the hydroponic solution was much smaller than that internalized by poplars (Table 2 and Figure 5C), suggesting that most of the internalized Cd taken up as QDs rather than as released Cd ions. QDs loosely adsorbed on the root surface were collected by multiple washing with DI water; this fraction was relatively small (about 3.5% for roots exposed to PEI-QDs and 1% for roots exposed to PAA-EG-QDs on day 2, Table 2), corroborating that Cd removed from hydroponic solution was mainly internalized by the poplars. Only a slight increase in total Cd and Se accumulation was observed after 11 days (2,457 ± 858 ng Cd/mg root and 1,059 ± 282 ng Se/mg root for poplars exposed to PEI-QDs versus 196 ± 54 ng Cd/mg

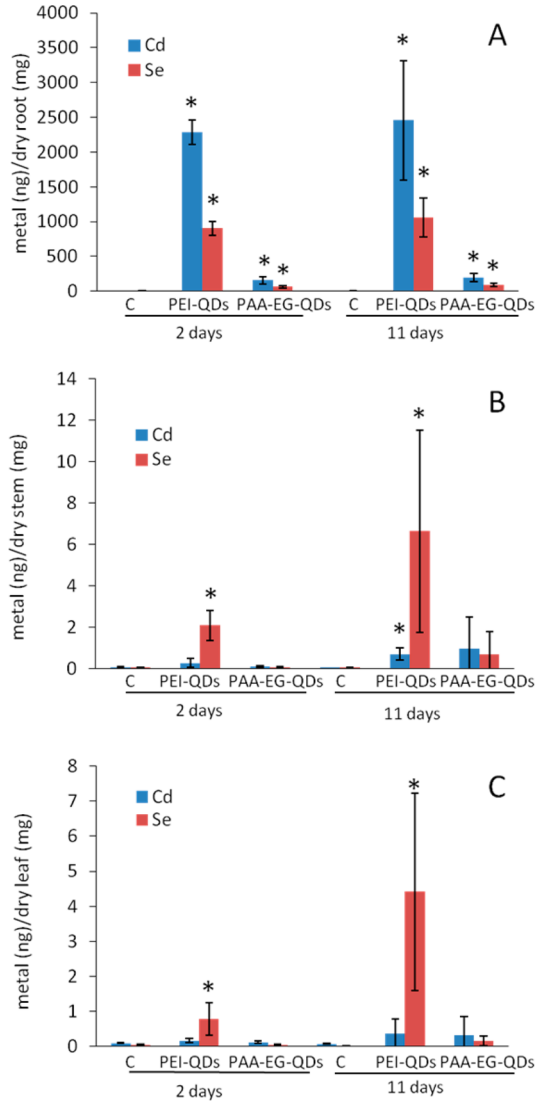

Figure 4. Cd and Se concentration in poplar root (A), stem (B), and leaf (C) after exposed to PEI-QDs or PAA-EG-QDs for 2 and 11 days. Stars (*) denote the statistically significant accumulation of Cd or Se in treated poplar tissues compared to the unexposed controls ($p < 0.05$). The significantly higher concentration of Se in stems and leaves of poplars exposed to PEI-QDs than in unexposed controls was probably due to the translocation of Se ions released from PEI-QDs. Error bars represent ±1 standard deviation ($n = 5$).

Table 2. Percentage of Cd and Se Remaining in Hydroponic Medium and Attaching on Root Surface after 2- and 11-Day Exposure[a]

		hydroponic medium		root surface	
QDs	time (days)	Cd	Se	Cd	Se
PEI-QDs	2	36.6 ± 16.8	27.9 ± 8.0	3.5 ± 2.1	3.5 ± 2.9
	11	12.4 ± 10.5	7.8 ± 5.3	3.2 ± 1.6	2.8 ± 1.8
PAA-EG-QDs	2	91.1 ± 2.0	76.5 ± 6.7	0.9 ± 0.2	0.6 ± 0.4
	11	87.3 ± 3.8	72.9 ± 10.8	1.0 ± 0.2	0.8 ± 0.2

[a]For each group, $n = 3$ and values are averages ±1 standard deviation.

dx.doi.org/10.1021/es501425r | Environ. Sci. Technol. 2014, 48, 6754−6762

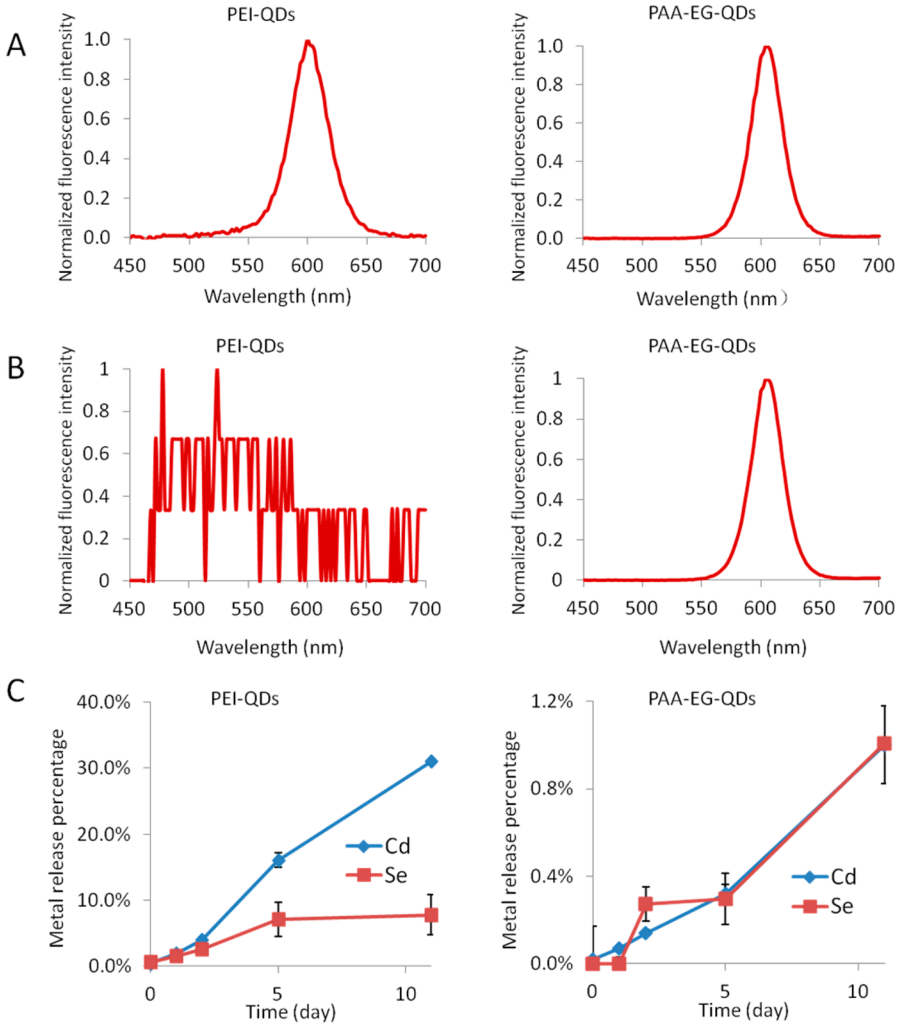

Figure 5. QD stability in 1/4-strength Hoagland solution during 11-day incubation. (A) QD fluorescence spectra on day 0. (B) QD fluorescence spectra on day 11. (C) Release percentage (released metal mass/total metal mass added) of Cd and Se from QDs during the incubation. The excitation wavelength was 401 nm. For (C), error bars represent ±1 standard deviation (n = 3).

root and 89 ± 26 ng Se/mg root for poplars exposed to PAA-EG-QDs), indicating a decrease in uptake rate over time (Figure 4A).

It is unlikely that the amino groups in the cationic coating (PEI) used in this study and in previous studies with herbaceous plants[12,22] significantly encouraged uptake as N source for plant growth, because the abundant NH_4^+ (1 mM) and NO_3^- (3.5 mM) present in the 1/4-strength Hoagland solution accounted for 96% of the total nitrogen in the medium. Nevertheless, the presence of some forms of nitrogen in NP coatings may influence uptake in nitrogen-limited systems. For example, Whiteside et al. conjugated different amino acids to commercial carboxyl QDs and tracked their uptake by annual bluegrass (*Poa annua*).[34] They found that QD-glycine (labile organic nitrogen) was taken up and translocated by bluegrass, while QD-chitosan (recalcitrant organic nitrogen) or bare QDs were not internalized.

Neither Anionic nor Cationic QDs Were Significantly Translocated to Poplar Shoots. The lack of detection of Cd and Se in shoot tissues of poplars exposed hydroponically to PAA-EG-QDs demonstrated their inefficient translocation from roots to shoots, while the low levels of Cd and Se detected in leaves and stems of poplars exposed to PEI-QDs suggests that (unlike uptake) translocation occurred mainly in the form of released ions rather than QDs (Figure 4B–C). For the PAA-EG-QD treatment, accumulation of Cd and Se in poplar shoots was insignificant on day 11 (p > 0.05, Figure 4B–C), even though confocal microscopy showed that some PAA-EG-QDs reached the stele through the endodermis (Figure 3A-B); this indicates slow translocation of QDs through the vascular system. For PEI-QDs, accumulation of Cd in poplar shoots after 11 days was only observed in stems (p < 0.05), but the measured concentration (0.7 ± 0.3 ng Cd/mg stem, Figure 4B) was close to detection limit (0.1 ng Cd/mg tissue) and the translocated amount only accounted for 0.1% of the total Cd (Table S1).

The Se concentrations in the shoots of poplars exposed to PEI-QDs were much higher than for Cd. The Se concentration in stems of poplars exposed to PEI-QDs was 6.6 ± 4.9 ng/mg tissue and in leaf 4.4 ± 2.8 ng/mg tissue on day 11, compared to 0.6 ± 0.3 ng/mg stem and 0.4 ± 0.4 ng/mg leaf for Cd (Figure 4B-C), even though the Cd (70.5 ± 0.6 μg/nmol PEI-QDs) content in original PEI-QDs core was four times higher than that of Se (17.8 ± 0.4 μg/nmol PEI-QDs). The preferential translocation of Se over Cd is corroborated by comparing the molar ratio of Cd/Se in poplar shoots. It was

dx.doi.org/10.1021/es501425r | Environ. Sci. Technol. 2014, 48, 6754–6762

0.09 ± 0.06 in stem and 0.06 ± 0.04 in leaf on day 11, both of which was remarkably lower than the original Cd/Se molar ration (2.79 ± 0.09) in PEI-QDs (Table S2). Note that about 7.8% of the Se in PEI-QDs was released from in the hydroponic solution during 11-day incubation (Figure 5C). Therefore, we infer that most of the Se detected in the shoots of poplars exposed to PEI-QDs was translocated as Se ions or organic Se released from QDs rather than as QDs. Some forms of Se (e.g., selenite and selenomethionine) have been confirmed to be effectively translocated to shoots in various plant species including poplar.[50−52]

The translocation of QDs to poplar shoots was likely hindered by the endodermis, which is the main barrier for the apoplastic transport of water and dissolved ions from outside solution into the root stele.[53] The Casparian strip of the endodermis, mainly consisting lignin polymer, makes the cell wall more hydrophobic and blocks the passive diffusion of solutes.[54,55] Thus, water and dissolved ions must transport through the protoplast of endodermal cells to reach the stele.[56] This transport process could be very challenging for the relatively large QD aggregates. Confocal images of roots exposed to PEI-QDs for 11 days show QD aggregates accumulating around the endodermis (Figure 3D-E and 3G-H). These QDs or their aggregates may be driven to the endodermis by the water flow toward the stele and failed to pass through the endodermis.

In contrast, for herbaceous plants, translocation of Au NPs was observed in several species, and negatively charged coating was reported to enhance translocation compared to neutral or positively charged coatings.[12,22] Higher difficulty for NPs to be translocated in woody poplars was probably due to its more differentiated tissues compared to herbaceous plants. For example, the NPs would have to pass through a thicker cortex in the poplar root to the endodermis (with casparian strip) to the xylem and from the xylem to woody stems and leaves.

Both Types of QDs Were Transformed Inside Poplar Roots. Regardless of coatings, the fluorescent properties of QDs are determined only by the size of the metallic core, with bigger cores emitting higher wavelengths.[4,57] In these experiments, the same size of metallic core was used for both types of QDs, and thus they exhibited identical fluorescence (Figure 5A). After 2-day exposure, the fluorescence emission peak of both PEI and PAA-EG coated QDs in poplar roots similarly red-shifted from 600 to 670 nm (Figure 2C and 3C). This "red-shift" indicates that part of the organic coating on QDs surface may have been lost inside the plant and the destabilized metallic core may have aggregated.

The two types of QDs exhibited different relative stabilities inside the plants versus in the hydroponic medium. For PEI-QDs, the fluorescence of their aggregates inside the plant was relatively stable throughout the exposure period (Figure 2D-E and 2G-H), while in 1/4-strength Hoagland solution, PEI-QDs were quenched after 11-day incubation (Figure 5B). The fluorescence intensity from roots exposed to these NPs also decreased with time (Figure S2D-F), suggesting loss of the coating and subsequent destabilization of PEI-QDs on root surfaces similarly as in the exposure medium. In contrast, PAA-EG-QDs were very stable in the exposure medium (Figure 5B); the fluorescence intensity from the roots increased with exposure time (Figure S2G-I), suggesting that PAA-EG-QDs may also be stable on the root surface. However, the 670 nm fluorescence emission from PAA-EG-QD aggregates, which was observed in the exposed root on day 2, disappeared by day 11 (Figure 3D-I). Since ICP-MS analysis showed that most of the internalized QD metals remained in the root (Figure 4), most of the PAA-EG-QD aggregates detected on day 2 must have been quenched by day 11.

Plant metabolism of xenobiotic organic compounds has been extensively studied for more than 70 years, and the associated detoxification or elimination processes have been conceptualized by the "green liver" model.[23,24] Specifically, internalized hydrophobic contaminants can be enzymatically transformed to hydrophilic compounds (e.g., by cytochrome P450) and subsequently conjugated by a macromolecule such as D-glucose, glutathione, and amino acids. The conjugate is then sequestered into the cell wall, vacuole, or lignin by covalent bonding, which compartmentalizes the substance out of the biochemical processing of plant cells.[23,24] While QDs are not dissolved contaminants, they are likewise foreign constituents exposed to similar biochemical environments upon uptake. We postulate that when fluorescent QDs enter into plant roots, their coatings may be susceptible to transformation, conjugation, and sequestration processes used by plants to process xenobiotic contaminants. Enzymes such as glutathione S-transferases (GSTs) involved in xenobiotic conjugation interact with compounds based on their functional groups,[24] and similar interactions may also apply for QD coatings. The amino groups in PEI and carboxyl groups in PAA-EG may interact with different biomolecules, possibly leading to different phytotransformation propensity of the two types of QDs used in this study.

Fluorescence from QDs or their aggregates is sensitive to surface modification, which could either stabilize the fluorescence by protecting the core from dissolution as manufactured organic coatings do, or quench it through redox-reactions, binding of the quencher, or hydrolysis of surface coating, depending on the specific conjugating biomolecules. Various biochemical compounds, such as amino acids, nucleotides, and DNA, can quench QD fluorescence irreversibly.[58] For example, elimination of CdTe QD fluorescence in freshwater alga cells (*Ochromonas danica*) was attributed to surface modification induced by amino acids and proteins in the vacuoles.[35] Potential differences in conjugation processes for PEI and PAA-EG coated QDs could cause the stabilization of the former aggregates and the quenching of the latter. Further research is needed to determine whether different coatings induce different plant responses and conjugating molecules, which is plausible since some plant metabolic enzymes such as GSTs are known to be induced by specific chemical compounds such as naphthalic anhydride and benoxacor.[23]

In summary, easier uptake of cationic PEI-QDs than anionic PAA-EG-QDs by woody poplars was likely facilitated by electrostatic attraction to the negatively charged cell wall. Further translocation to shoots was hindered by aggregation upon destabilization of the organic coatings, which delayed or precluded passage through the endodermis. Moreover, transformation of QDs within plants could either stabilize or quench their fluorescence, and the propensity for such phytotransformations is not necessarily reflected by their stability in the hydroponic medium. Overall, these findings suggest that plant uptake and bioaccumulation of manufactured NPs could be mitigated (along with the associated introduction into food webs) through appropriate selection of manipulation of the charge and stability (e.g., propensity for hydrolysis or enzymatic attack) of surface coatings.

■ ASSOCIATED CONTENT

Supporting Information

Details on ICP-MS analysis, confocal images of control root sections, cumulative evapotranspiration data, and fluorescent images of poplar root. This material is available free of charge via the Internet at http://pubs.acs.org.

■ AUTHOR INFORMATION

Corresponding Author

*Phone: (713)348-5903. E-mail: alvarez@rice.edu.

Notes

The authors declare no competing financial interest.

■ ACKNOWLEDGMENTS

This research was supported by the National Science Foundation (CMMI-1057906). Jing Wang also received partial support from a scholarship from the China Scholarship Council. We thank Dr. A. Budi Utama for his assistance with Confocal Microscopy, Dr. Xiangyu Wang for her help with cryosection sample preparation, and Dr. Nastassja A. Lewinski for her advice on cryosection sample preparation.

■ REFERENCES

(1) Gao, X.; Cui, Y.; Levenson, R. M.; Chung, L. W.; Nie, S. *In vivo* cancer targeting and imaging with semiconductor quantum dots. *Nat. Biotechnol.* **2004**, *22* (8), 969−976.

(2) Loss, D.; DiVincenzo, D. P. Quantum computation with quantum dots. *Phys. Rev. A* **1998**, *57* (1), 120.

(3) Mora-Seró, I.; Gimenez, S.; Fabregat-Santiago, F.; Gomez, R.; Shen, Q.; Toyoda, T.; Bisquert, J. Recombination in quantum dot sensitized solar cells. *Acc. Chem. Res.* **2009**, *42* (11), 1848−1857.

(4) Medintz, I. L.; Uyeda, H. T.; Goldman, E. R.; Mattoussi, H. Quantum dot bioconjugates for imaging, labelling and sensing. *Nat. Mater.* **2005**, *4* (6), 435−446.

(5) Ballou, B.; Lagerholm, B. C.; Ernst, L. A.; Bruchez, M. P.; Waggoner, A. S. Noninvasive imaging of quantum dots in mice. *Bioconjugate Chem.* **2004**, *15* (1), 79−86.

(6) Lewinski, N. A.; Zhu, H.; Jo, H.-J.; Pham, D.; Kamath, R. R.; Ouyang, C. R.; Vulpe, C. D.; Colvin, V. L.; Drezek, R. A. Quantification of water solubilized CdSe/ZnS quantum dots in *Daphnia magna*. *Environ. Sci. Technol.* **2010**, *44* (5), 1841−1846.

(7) Kloepfer, J.; Mielke, R.; Nadeau, J. Uptake of CdSe and CdSe/ZnS quantum dots into bacteria via purine-dependent mechanisms. *Appl. Environ. Microbiol.* **2005**, *71* (5), 2548−2557.

(8) Schroeder, J.; Shweky, I.; Shmeeda, H.; Banin, U.; Gabizon, A. Folate-mediated tumor cell uptake of quantum dots entrapped in lipid nanoparticles. *J. Controlled Release* **2007**, *124* (1), 28−34.

(9) Kim, S.; Fisher, B.; Eisler, H.-J.; Bawendi, M. Type-II quantum dots: CdTe/CdSe (core/shell) and CdSe/ZnTe (core/shell) heterostructures. *J. Am. Chem. Soc.* **2003**, *125* (38), 11466−11467.

(10) Michalet, X.; Pinaud, F. F.; Bentolila, L. A.; Tsay, J. M.; Doose, S.; Li, J. J.; Sundaresan, G.; Wu, A. M.; Gambhir, S. S.; Weiss, S. Quantum dots for live cells, *in vivo* imaging, and diagnostics. *Science* **2005**, *307* (5709), 538−544.

(11) Shashkov, E. V.; Everts, M.; Galanzha, E. I.; Zharov, V. P. Quantum dots as multimodal photoacoustic and photothermal contrast agents. *Nano Lett.* **2008**, *8* (11), 3953−3958.

(12) Zhu, Z.; Wang, H.; Yan, B.; Zheng, H.; Jiang, Y.; Miranda, O. R.; Rotello, V. M.; Xing, B.; Vachet, R. W. Effect of surface charge on the uptake and distribution of gold nanoparticles in four plant species. *Environ. Sci. Technol.* **2012**, *46* (22), 12391−12398.

(13) Sabo-Attwood, T.; Unrine, J. M.; Stone, J. W.; Murphy, C. J.; Ghoshroy, S.; Blom, D.; Bertsch, P. M.; Newman, L. A. Uptake, distribution and toxicity of gold nanoparticles in tobacco (*Nicotiana xanthi*) seedlings. *Nanotoxicology* **2012**, *6* (4), 353−360.

(14) Zhai, G.; Walters, K. S.; Peate, D. W.; Alvarez, P. J.; Schnoor, J. L. Transport of gold nanoparticles through plasmodesmata and precipitation of gold ions in woody poplar. *Environ. Sci. Technol. Lett.* **2014**, *1* (2), 146−151.

(15) Doshi, R.; Braida, W.; Christodoulatos, C.; Wazne, M.; O'Connor, G. Nano-aluminum: Transport through sand columns and environmental effects on plants and soil communities. *Environ. Res.* **2008**, *106* (3), 296−303.

(16) Lopez-Moreno, M. L.; de la Rosa, G.; Hernandez-Viezcas, J. A.; Peralta-Videa, J. R.; Gardea-Torresdey, J. L. X-ray absorption spectroscopy (XAS) corroboration of the uptake and storage of CeO_2 nanoparticles and assessment of their differential toxicity in four edible plant species. *J. Agric. Food Chem.* **2010**, *58* (6), 3689−3693.

(17) Birbaum, K.; Brogioli, R.; Schellenberg, M.; Martinoia, E.; Stark, W. J.; Günther, D.; Limbach, L. K. No evidence for cerium dioxide nanoparticle translocation in maize plants. *Environ. Sci. Technol.* **2010**, *44* (22), 8718−8723.

(18) Servin, A. D.; Castillo-Michel, H.; Hernandez-Viezcas, J. A.; Diaz, B. C.; Peralta-Videa, J. R.; Gardea-Torresdey, J. L. Synchrotron micro-XRF and micro-XANES confirmation of the uptake and translocation of TiO_2 nanoparticles in cucumber (*Cucumis sativus*) plants. *Environ. Sci. Technol.* **2012**, *46* (14), 7637−7643.

(19) Kurepa, J.; Paunesku, T.; Vogt, S.; Arora, H.; Rabatic, B. M.; Lu, J.; Wanzer, M. B.; Woloschak, G. E.; Smalle, J. A. Uptake and distribution of ultrasmall anatase TiO_2 Alizarin red S nanoconjugates in *Arabidopsis thaliana*. *Nano Lett.* **2010**, *10* (7), 2296−2302.

(20) Hernandez-Viezcas, J. A.; Castillo-Michel, H.; Andrews, J. C.; Cotte, M.; Rico, C.; Peralta-Videa, J. R.; Ge, Y.; Priester, J. H.; Holden, P. A.; Gardea-Torresdey, J. L. In situ synchrotron X-ray fluorescence mapping and speciation of CeO_2 and ZnO nanoparticles in soil cultivated soybean (*Glycine max*). *ACS Nano* **2013**, *7* (2), 1415−1423.

(21) Servin, A. D.; Morales, M. I.; Castillo-Michel, H.; Hernandez-Viezcas, J. A.; Munoz, B.; Zhao, L.; Nunez, J. E.; Peralta-Videa, J. R.; Gardea-Torresdey, J. L. Synchrotron verification of TiO_2 accumulation in cucumber fruit: a possible pathway of TiO_2 nanoparticle transfer from soil into the food chain. *Environ. Sci. Technol.* **2013**, *47* (20), 11592−11598.

(22) Koelmel, J.; Leland, T.; Wang, H.; Amarasiriwardena, D.; Xing, B. Investigation of gold nanoparticles uptake and their tissue level distribution in rice plants by laser ablation-inductively coupled-mass spectrometry. *Environ. Pollut.* **2013**, *174*, 222−228.

(23) Sandermann, H., Jr. Higher plant metabolism of xenobiotics: the 'green liver' concept. *Pharmacogenet. Genomics* **1994**, *4* (5), 225−241.

(24) Burken, J. Uptake and metabolism of organic compounds: green-liver model. In *Phytoremediation: transformation and control of contaminants*; McCutcheon, S. C., Schnoor, J. L., Eds.; John Wiley & Sons, Inc.: Hoboken, NJ, 2003; p 59.

(25) Briggs, G. G.; Bromilow, R. H.; Evans, A. A. Relationships between lipophilicity and root uptake and translocation of non-ionised chemicals by barley. *Pestic. Sci.* **1982**, *13* (5), 495−504.

(26) Burken, J. G.; Schnoor, J. L. Predictive relationships for uptake of organic contaminants by hybrid poplar trees. *Environ. Sci. Technol.* **1998**, *32* (21), 3379−3385.

(27) Dimkpa, C.; McLean, J.; Latta, D.; Manangón, E.; Britt, D.; Johnson, W.; Boyanov, M.; Anderson, A. CuO and ZnO nanoparticles: phytotoxicity, metal speciation, and induction of oxidative stress in sand-grown wheat. *J. Nanopart. Res.* **2012**, *14* (9), 1−15.

(28) Wang, Z.; Xie, X.; Zhao, J.; Liu, X.; Feng, W.; White, J. C.; Xing, B. Xylem- and phloem-based transport of CuO nanoparticles in maize (*Zea mays* L.). *Environ. Sci. Technol.* **2012**, *46* (8), 4434−4441.

(29) Lopez-Moreno, M. L.; de la Rosa, G.; Hernandez-Viezcas, J. A.; Castillo-Michel, H.; Botez, C. E.; Peralta-Videa, J. R.; Gardea-Torresdey, J. L. Evidence of the differential biotransformation and genotoxicity of ZnO and CeO_2 nanoparticles on soybean (*Glycine max*) plants. *Environ. Sci. Technol.* **2010**, *44* (19), 7315−7320.

(30) Parsons, J. G.; Lopez, M. L.; Gonzalez, C. M.; Peralta-Videa, J. R.; Gardea-Torresdey, J. L. Toxicity and biotransformation of uncoated and coated nickel hydroxide nanoparticles on mesquite plants. *Environ. Toxicol. Chem.* **2010**, *29* (5), 1146−1154.

(31) Ma, Y.; He, X.; Zhang, P.; Zhang, Z.; Guo, Z.; Tai, R.; Xu, Z.; Zhang, L.; Ding, Y.; Zhao, Y.; Chai, Z. Phytotoxicity and biotransformation of La_2O_3 nanoparticles in a terrestrial plant cucumber (*Cucumis sativus*). *Nanotoxicology* **2011**, *5* (4), 743−753.
(32) Zhang, P.; Ma, Y.; Zhang, Z.; He, X.; Guo, Z.; Tai, R.; Ding, Y.; Zhao, Y.; Chai, Z. Comparative toxicity of nanoparticulate/bulk Yb_2O_3 and $YbCl_3$ to cucumber (*Cucumis sativus*). *Environ. Sci. Technol.* **2011**, *46* (3), 1834−1841.
(33) Zhang, P.; Ma, Y.; Zhang, Z.; He, X.; Zhang, J.; Guo, Z.; Tai, R.; Zhao, Y.; Chai, Z. Biotransformation of ceria nanoparticles in cucumber plants. *ACS Nano* **2012**, *6* (11), 9943−9950.
(34) Whiteside, M. D.; Treseder, K. K.; Atsatt, P. R. The brighter side of soils: quantum dots track organic nitrogen through fungi and plants. *Ecology* **2009**, *90* (1), 100−108.
(35) Wang, Y.; Miao, A.-J.; Luo, J.; Wei, Z.-B.; Zhu, J.-J.; Yang, L.-Y. Bioaccumulation of CdTe quantum dots in a freshwater alga *Ochromonas danica*: A kinetics study. *Environ. Sci. Technol.* **2013**, *47* (18), 10601−10610.
(36) Zhu, H.; Prakash, A.; Benoit, D. N.; Jones, C. J.; Colvin, V. L. Low temperature synthesis of ZnS and CdZnS shells on CdSe quantum dots. *Nanotechnology* **2010**, *21* (25), 255604.
(37) Yang, Y.; Zhu, H.; Colvin, V. L.; Alvarez, P. J. Cellular and transcriptional response of *Pseudomonas stutzeri* to quantum dots under aerobic and denitrifying conditions. *Environ. Sci. Technol.* **2011**, *45* (11), 4988−4994.
(38) Hoagland, D. R.; Arnon, D. I. The water-culture method for growing plants without soil. *Circ. - Calif. Agric. Exp. Stn.* **1950**, *347*.
(39) Wang, J.; Koo, Y.; Alexander, A.; Yang, Y.; Westerhof, S.; Zhang, Q.; Schnoor, J. L.; Colvin, V. L.; Braam, J.; Alvarez, P. J. Phytostimulation of poplars and *Arabidopsis* exposed to silver nanoparticles and Ag^+ at sublethal concentrations. *Environ. Sci. Technol.* **2013**, *47* (10), 5442−5449.
(40) Xiu, Z.-m.; Gregory, K. B.; Lowry, G. V.; Alvarez, P. J. Effect of bare and coated nanoscale zerovalent iron on *tceA* and *vcrA* gene expression in *Dehalococcoides* spp. *Environ. Sci. Technol.* **2010**, *44* (19), 7647−7651.
(41) Mahendra, S.; Zhu, H.; Colvin, V. L.; Alvarez, P. J. Quantum dot weathering results in microbial toxicity. *Environ. Sci. Technol.* **2008**, *42* (24), 9424−9430.
(42) Phenrat, T.; Saleh, N.; Sirk, K.; Kim, H.-J.; Tilton, R. D.; Lowry, G. V. Stabilization of aqueous nanoscale zerovalent iron dispersions by anionic polyelectrolytes: adsorbed anionic polyelectrolyte layer properties and their effect on aggregation and sedimentation. *J. Nanopart. Res.* **2008**, *10* (5), 795−814.
(43) Saleh, N.; Phenrat, T.; Sirk, K.; Dufour, B.; Ok, J.; Sarbu, T.; Matyjaszewski, K.; Tilton, R. D.; Lowry, G. V. Adsorbed triblock copolymers deliver reactive iron nanoparticles to the oil/water interface. *Nano Lett.* **2005**, *5* (12), 2489−2494.
(44) Saleh, N.; Sarbu, T.; Sirk, K.; Lowry, G. V.; Matyjaszewski, K.; Tilton, R. D. Oil-in-water emulsions stabilized by highly charged polyelectrolyte-grafted silica nanoparticles. *Langmuir* **2005**, *21* (22), 9873−9878.
(45) Yang, X.; Gondikas, A. P.; Marinakos, S. M.; Auffan, M.; Liu, J.; Hsu-Kim, H.; Meyer, J. N. Mechanism of silver nanoparticle toxicity is dependent on dissolved silver and surface coating in *Caenorhabditis elegans*. *Environ. Sci. Technol.* **2011**, *46* (2), 1119−1127.
(46) Phenrat, T.; Cihan, A.; Kim, H.-J.; Mital, M.; Illangasekare, T.; Lowry, G. V. Transport and deposition of polymer-modified Fe^0 nanoparticles in 2-D heterogeneous porous media: Effects of particle concentration, Fe^0 content, and coatings. *Environ. Sci. Technol.* **2010**, *44* (23), 9086−9093.
(47) Lazof, D. B.; Goldsmith, J. G.; Rufty, T. W.; Linton, R. W. Rapid uptake of aluminum into cells of intact soybean root tips (a microanalytical study using secondary ion mass spectrometry). *Plant Physiol.* **1994**, *106* (3), 1107−1114.
(48) Grignon, C.; Sentenac, H. pH and ionic conditions in the apoplast. *Annu. Rev. Plant Biol.* **1991**, *42* (1), 103−128.
(49) Wehr, J. B.; Blamey, F. P. C.; Menzies, N. W. Comparison between methods using copper, lanthanum, and colorimetry for the determination of the cation exchange capacity of plant cell walls. *J. Agric. Food Chem.* **2010**, *58* (8), 4554−4559.
(50) Pilon-Smits, E.; De Souza, M.; Lytle, C.; Shang, C.; Lugo, T.; Terry, N. Selenium volatilization and assimilation by hybrid poplar (*Populus tremula x alba*). *J. Exp. Bot.* **1998**, *49* (328), 1889−1892.
(51) Bañuelos, G.; Shannon, M.; Ajwa, H.; Draper, J.; Jordahl, J.; Licht, J. Phytoextraction and accumulation of boron and selenium by poplar (*Populus*) hybrid clones. *Int. J. Phytoremediat.* **1999**, *1* (1), 81−96.
(52) Terry, N.; Zayed, A.; De Souza, M.; Tarun, A. Selenium in higher plants. *Annu. Rev. Plant Biol.* **2000**, *51* (1), 401−432.
(53) Schreiber, L.; Hartmann, K.; Skrabs, M.; Zeier, J. Apoplastic barriers in roots: chemical composition of endodermal and hypodermal cell walls. *J. Exp. Bot.* **1999**, *50* (337), 1267−1280.
(54) Naseer, S.; Lee, Y.; Lapierre, C.; Franke, R.; Nawrath, C.; Geldner, N. Casparian strip diffusion barrier in *Arabidopsis* is made of a lignin polymer without suberin. *Proc. Natl. Acad. Sci. U.S.A.* **2012**, *109* (25), 10101−10106.
(55) Nagahashi, G.; Thomson, W.; Leonard, R. The Casparian strip as a barrier to the movement of lanthanum in corn roots. *Science* **1974**, *183* (4125), 670−671.
(56) Clarkson, D.; Robards, A. The endodermis, its structural development and physiological role. In *The development and function of roots*; Academic Press: *Hordeum, Zea. J. Tissues_end, Plasmodesmata Ectodesmata, Transloc, Poaceae Gramineae, Ultrastr_tem., Review article General article, Roots (PMBD, 185602030)*, 1975.
(57) Dabbousi, B.; Rodriguez-Viejo, J.; Mikulec, F. V.; Heine, J.; Mattoussi, H.; Ober, R.; Jensen, K.; Bawendi, M. CdSe) ZnS core-shell quantum dots: synthesis and characterization of a size series of highly luminescent nanocrystallites. *J. Phys. Chem. B* **1997**, *101* (46), 9463−9475.
(58) Siegberg, D.; Herten, D.-P. Fluorescence quenching of quantum dots by DNA nucleotides and amino acids. *Aust. J. Chem.* **2011**, *64* (5), 512−516.